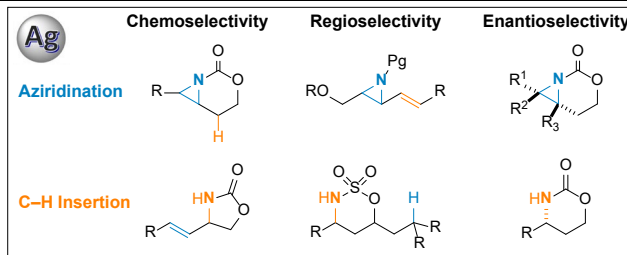


# Tunable Silver-Catalyzed Nitrene Transfer: From Chemoselectivity to Enantioselective C–H Amination

Wentan Liu,<sup>†</sup> Isaac Choi,<sup>†</sup> Emily E. Zerull, and Jennifer M. Schomaker\*

University of Wisconsin, Department of Chemistry, 1101 University Avenue, Madison, WI 53706, USA

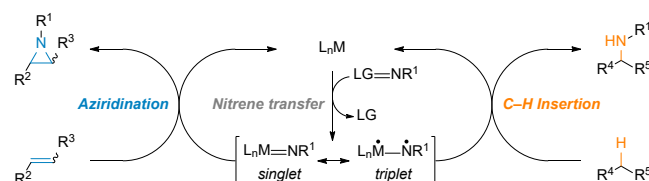


**ABSTRACT:** Transition metal-catalyzed C–H aminations *via* nitrene transfer processes are powerful synthetic methods to construct valuable amines. Over the last decade, significant efforts in the field have resulted in an expansion in the utility of nitrene transfer chemistry, enabling the use of these carbon–nitrogen bond forming reactions in complex organic molecule syntheses. This Perspective highlights efforts in silver-catalyzed nitrene transfer reactions that achieve chemo-, site- and enantioselective transformations using simple *N*-determinate ligands that can serve as steppingstones for future investigations in other tunable C–H functionalizations.

**Keywords:** nitrene transfer, C–N bond formation, silver catalysis, enantioselectivity, amination, amines, aziridines, C–H functionalization

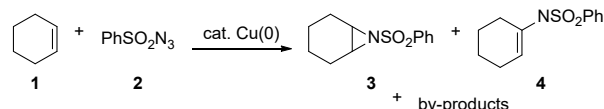
## 1 Introduction

Transition metal-catalyzed nitrene transfer (NT) reactions have received significant attention as robust methods to prepare amine scaffolds that are useful for the synthesis of agricultural chemicals, drugs, chiral amine ligands and for monomers used in materials science. Thus, nitrene transfer reactions have been studied with many transition metals, with Rh, Ru, Ir, Cu, Fe, Co, Mn, and Ag among the most extensively researched.<sup>1–14</sup> The general mechanism for the nitrene transfer process involves the reaction of a ligand–metal complex with an oxidized nitrene precursor to form the metal-supported reactive species. The resulting singlet or triplet nitrene intermediate then engages in the formation of a new carbon–nitrogen bond through a subsequent addition or insertion into either a C=C or C–H bond, respectively (Scheme 1).



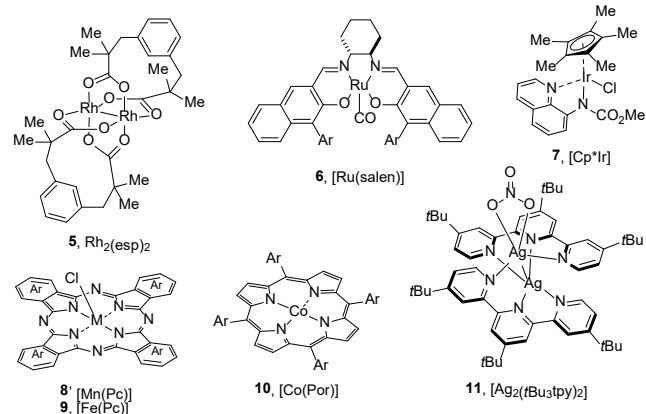
**Scheme 1.** General proposed mechanism for metal-catalyzed nitrene transfer reactions.

The chemistry of metallonitrenes can be traced back to 1967 when Kwart and Khan first described the Cu(0)-catalyzed decomposition of benzosulfonyl azides, which was followed by subsequent formation of aziridines and vinyl amines (Scheme 2).<sup>15</sup>



**Scheme 2.** The first reported nitrene transfer reaction.

In the intervening years, a number of transition metal complexes have been developed for effective nitrene transfer (Scheme 3). Precious metals such as rhodium,<sup>16</sup> ruthenium,<sup>17–19</sup> and iridium<sup>20,21</sup>, which have been extensively studied by the group of Du Bois, Katsuki, and Chang, respectively, show excellent catalytic activities in nitrene transfers that include C–H amination and aziridination.<sup>16</sup> A number of 3d metal complexes, such as

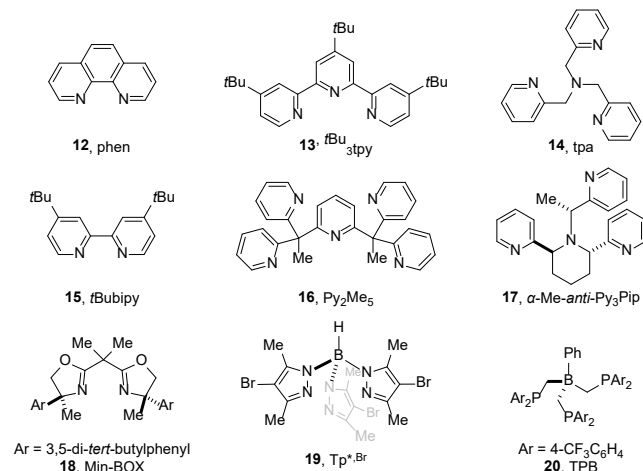


**Scheme 3.** Various metal catalysts employed for nitrene transfer reactions.

those based on manganese (**8**), iron (**9**), and cobalt (**10**), provide similar reaction outcomes when supported by

tetridentate ligands.<sup>22-28</sup> Silver has also proven to be a good metal to promote nitrene transfer. In 2003, the He group reported the first silver-catalyzed nitrene transfer reaction, in which dinuclear silver complex **11** enabled the aziridination of different olefins.<sup>29</sup>

Based on the seminal work by the Hu group, the Schomaker and Pérez groups have recently presented remarkable results in silver-catalyzed nitrene transfer reactions. In particular, they have revealed how the use of a diverse range of *N*-dentine ligands **12-20** on silver enables predictable and selective NT (Scheme 4) across a broad range of substrates.



**Scheme 4.** Diverse ligands used in silver-catalyzed nitrene transfer.

The aim of this Perspective is to highlight how variations in the coordination environment around the metal center and control over the fluxional behavior of some silver complexes in solution can deliver new strategies to influence the chemo-, site-, and stereoselectivity of NT and inspire the further tailoring of ligands for silver- and other metal-catalyzed C-H functionalizations.

## 2 Chemoselective Nitrene Transfer

### 2.1 Intramolecular Chemoselective Nitrene Transfer

Achieving chemoselective NT in the presence of competing C-H and C=C bonds is challenging, especially when it is advantageous to employ a broad range of nitrene precursors. In this regard, the Schomaker group reported a chemoselective aziridination of homoallenic carbamates by changing only the ligand identity on AgOTf.<sup>30</sup> The use of bidentate ligands provided superior chemoselectivity for formation of the aziridine **22** (Table 1, Entries 1-5). In contrast, a 2,2';6',2"-terpyridine (terpy) ligand showed a switch in selectivity, affording cyclic carbamate **23** as the major product (Table 1, Entry 6), with a small amount of **22**.

The coordination chemistry of silver complexes can be strongly influenced by changes to the ligand character, the

**Table 1.** Chemoselective silver-catalyzed nitrene transfer reactions of carbamates.

Entry	Ligand	Aziridination	Insertion	A : I
1	phen	80%	14%	5.7 : 1
2	bathophen	84%	12%	7 : 1
3	bipy	68%	11%	6.2 : 1
4	p-OMe-bipy	73%	11%	6.6 : 1
5	p-Ph-bipy	62%	20%	3.1 : 1
6	terpy	9%	61%	1 : 6.8

metal:ligand ratio and even the counteranion of the silver salt.<sup>31-37</sup> In this regard, the Schomaker group was able to accomplish a chemoselective nitrene transfer similar to that in Table 1 by simply controlling the metal:ligand ratio. Indeed, different ratios of metal and ligand showed a dramatic alteration in the ratio of product formation, in which <1:2 ratio of AgOTf:phen **12** selected for the aziridine product **22**, while ratios >1:2 reversed the chemoselectivity to favor the C-H insertion product **23** (Table 2).

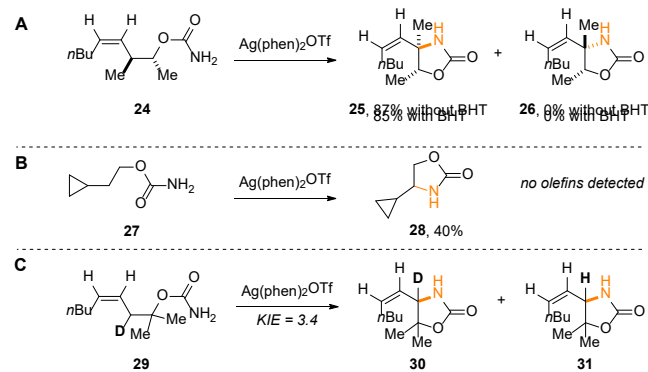
**Table 2.** Effect of metal:ligand ratio on chemoselectivity.

Entry	Ag : phen	Aziridination	C-H Insertion	A : I	Aziridination by	C-H Insertion by
1	1 : 0.5	60%	12%	5 : 1		
2	1 : 1	75%	13%	5.8 : 1		
3	1 : 1.25	80%	13%	6.2 : 1		
4	1 : 1.5	70%	12%	5.8 : 1		
5	1 : 2	18%	72%	1 : 4		
6	1 : 3	2%	76%	1 : 38		

As part of their mechanistic investigations, the Schomaker group noted that similar yields were observed in the presence or absence of a radical inhibitor. No alkene isomerization was seen and the stereochemistry of the original substrate was preserved during the course of the reaction (Scheme 5A). These experimental results provided strong support for a concerted C-H insertion mechanism, but could not rule out the presence of short-lived radical intermediates. Radical clock experiments suggested that a pathway involving long-lived radicals is not likely to be operative (Scheme 5B). A kinetic isotope effect (KIE) study also indicated that a concerted process for silver-catalyzed C-H amination (Scheme 5C) was a distinct possibility, as the KIE values were similar to those reported by Du Bois for Rh-catalyzed, concerted NT.<sup>38-40</sup> A possible rapid radical rebound mechanism was also considered, where single

hydrogen-transfer is followed by a barrierless radical recombination, but support for this pathway could only be obtained through computational studies.

**Scheme 5.** Stereochemical probes and KIE experiments.



Detailed reaction profiling showed that the rate of aziridination was decreased as the concentration of ligand was increased (Figure 1a), while a slight increase in the rate of C-H insertion was observed when a higher ligand concentration was employed (Figure 1b).<sup>41</sup>

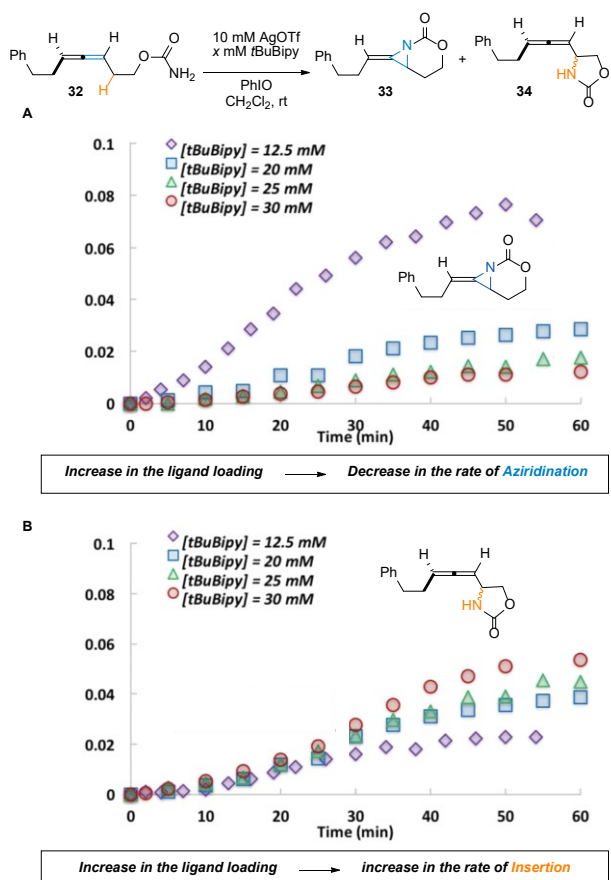
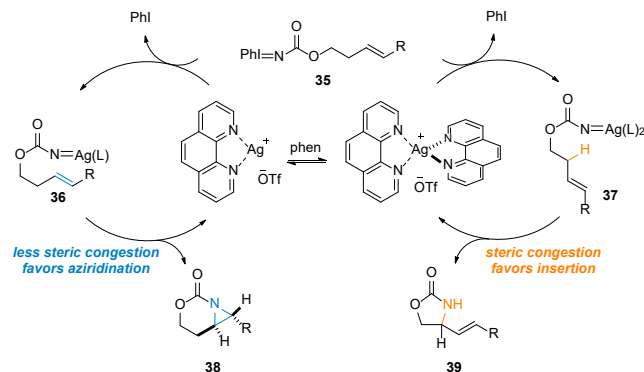


**Figure 1.** Kinetic profiling of aziridination vs. C-H insertion. Reprinted with permission from *Organometallics* 2017, 36, 1649-1661. Copyright © 2017, American Chemical Society.

Since the mono- and bis-ligated silver complexes showed similar reaction mechanisms based on experimental and computational studies, excellent chemoselectivity was presumably achieved by modulating steric hindrance at the silver center, leading to differences in the rate of each respective nitrene transfer event (Scheme 6).

**Scheme 6.** Proposed mechanism for divergent silver-catalyzed chemoselective amination.



## 2.2 Intermolecular Chemoselective Nitrene Transfer

Controlling chemoselectivity in intermolecular nitrene transfer can be especially challenging when multiple reactive sites are present. Although the Schomaker group attempted to apply their strategy for tunable chemoselectivity to intermolecular NT, no significant selectivity change was noted by altering the metal:ligand ratio. However, different ligand selections allowed for good control over chemoselectivity. The use of a *t*Bu<sub>3</sub>tpy ligand **13** selectively afforded aziridinated product **44** with hexafluoropropan-2-yl sulfamate (HfsNH<sub>2</sub>). On the other hand, pairing a tris(2-pyridylmethyl)amine (tpa) ligand **14** with 2,6-difluorophenyl sulfamate (DfsNH<sub>2</sub>) as a nitrene precursor preferentially gave allylic amination (Table 3).

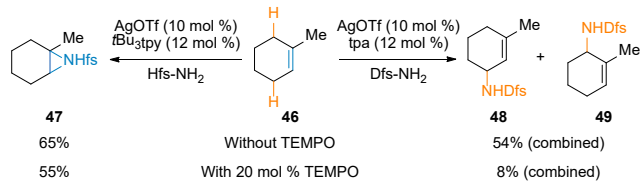
**Table 3.** Tunable, catalyst-controlled intermolecular chemoselective amination.

Entry	Substrate	Ligand	Aziridination*	C-H Insertion*	A : I
1		<i>t</i> Bu <sub>3</sub> tpy	84%	13%	<b>6.5</b> : 1
2		tpa	8%	46%	1 : <b>5.8</b>
3		<i>t</i> Bu <sub>3</sub> tpy	73%	7%	<b>10</b> : 1
4		tpa	7%	61%	1 : <b>8.7</b>
5		<i>t</i> Bu <sub>3</sub> tpy	58%	4%	<b>15</b> : 1
6		tpa	8%	25%	1 : <b>3.1</b>

Experimental mechanistic investigations were carried out to decipher the nature of these diverging silver-catalyzed

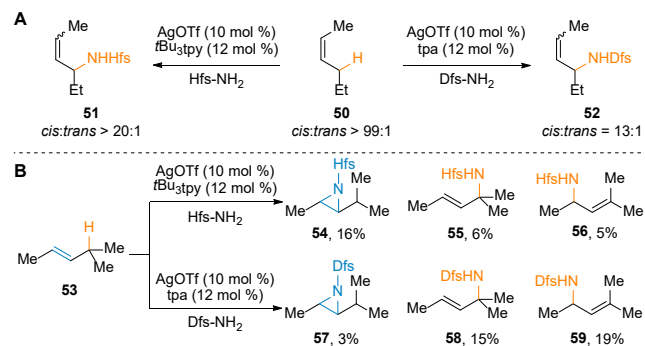
NT processes. Interestingly, reactions with TEMPO as a radical scavenger showed a clear difference in reactivity between the aziridination pathway and the C–N bond formation pathway (Scheme 7). Similar conversions to aziridine **47** were observed with and without the presence of TEMPO; in contrast, a significant suppression of product formation in the presence of the radical scavenger was detected in the C–H insertion process. These results imply that the two reactions may occur through different mechanisms and that the nature of the ligand may impact the lifetime of any radical intermediates.

**Scheme 7.** Experiments with TEMPO as a representative radical scavenger.



Interestingly, further intermolecular NT experiments using the acyclic *cis*-alkene **50** revealed that catalysts supported by both *tBu*<sub>3</sub>tpy **13** and tpa **14** afforded C–H amidated products, where the *cis* nature of the alkene was preserved in the major product (Scheme 8A). On the other hand, a double bond transposition was observed in the reactions of the same catalysts with alkene **53** (Scheme 8B). Thus, the involvement of radical intermediates in both silver-catalyzed reactions cannot be excluded on the basis of experimental results.

**Scheme 8.** Stereochemical probes and isomerization studies.



To gain a better understanding of the intermolecular silver-catalyzed NT chemistry, a crystallographic analysis of  $[(\text{tBu}_3\text{tpy})\text{AgOTf}]_2$  was conducted. A single crystal X-ray structure indicated the presence of two inequivalent silver atoms,  $\text{Ag}^1$  and  $\text{Ag}^2$ . The  $\text{Ag}^1$  is only coordinated to nitrogens of the *tBu*<sub>3</sub>tpy ligand **13**, while the  $\text{Ag}^2$  exhibits additional coordination with the triflate anion (Scheme 8A). A computational analysis of the putative nitrene intermediate indicated that the nitrene prefers to bind to  $\text{Ag}^1$  over  $\text{Ag}^2$  in the dimeric silver complex supported by a terpyridine

ligand as a simplified substitute for *tBu*<sub>3</sub>tpy **13** (Figure 2A). On the other hand, the monomeric silver complex with tpa **14**, suggested that the nitrene is bound at a pseudo-equatorial site on the metal center, with the triflate anion axially coordinated to the silver (Figure 2B). This suggests that the use of different ligands leads to a change in the trajectory by which a given nitrene precursor approaches the silver core; this can influence the chemoselectivity in intermolecular silver-catalyzed NT. Furthermore, based on detailed computational studies, two different nitrene transfer mechanisms were proposed. For the silver complex formed using *tBu*<sub>3</sub>tpy **13**, a semi-chelation mode allows for barrierless radical rebound due to an elongated silver–nitrogen bond in the hydrogen atom transfer (HAT) transition state, with enthalpy playing a major role in the aziridination pathway. For the silver complex supported by tpa **14**, a longer-lived radical intermediate was proposed, with entropy driving the preferential formation of the C–H amination product. This computational insight indirectly supports experimental results showing erosion of stereochemistry and a decrease in yield when a radical scavenger was utilized in the NT reaction.

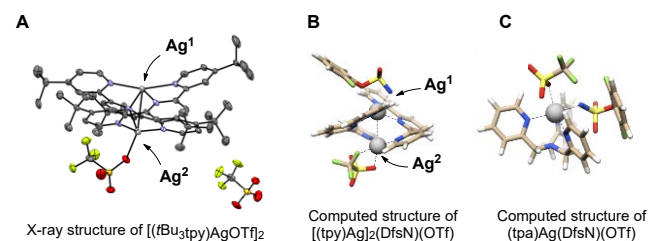


**Figure 2.** X-ray structure of  $[(\text{tBu}_3\text{tpy})\text{AgOTf}]_2$  and computationally calculated silver complexes with nitrene precursors. Reprinted with permission from *J. Am. Chem. Soc.* **2016**, *138*, 14658–14667. Copyright © 2016, American Chemical Society.

### 3 Regioselective Nitrene Transfer

#### 3.1 Intramolecular Regioselective Nitrene Transfer

Despite significant advances in nitrene transfer, the realization of a regioselective C–H amination controlled solely by the catalyst remains challenging. For this reason, tailoring catalysts that are able to discriminate between specific activated C–H bonds is highly desirable.

##### 3.1.1 Tertiary C(sp<sup>3</sup>)–H Bonds vs. Activated C–H Bonds

To address this challenge, the Schomaker group described silver-catalyzed regioselective C–H amidations that were capable of differentiating between an activated electron-rich tertiary C(sp<sup>3</sup>)–H bond (**T**) and an activated C(sp<sup>3</sup>)–H bond (**A**) (Table 4).<sup>43</sup> In their study, a silver catalyst supported by *tBu*bipy **15** preferred functionalization at **T**, while tpa **14** preferred amination at **A**, again showcasing the important role of ligands in tuning the site-selectivity of NT. Based on the selected examples in Table 4, the sterics did not affect the **T**-functionalization to any great extent (Table 4, Entries 1 and 3), but **A**-functionalization benefited from

increased steric hindrance at the competing sites (Table 4, Entries 2 and 4). Similarly, employing electron-withdrawing substituents on the aromatic ring resulted in an enhanced preference for **T**-functionalization (Table 4, Entry 5) and reversed the selectivity trend for C–H amination in **A**-functionalization (Table 4, Entry 6). For allylic and propargylic C–H bonds, similar trends in selectivity were observed (Table 4, Entries 7–10).

**Table 4.** Regioselective C–H amination between tertiary and activated C–H bonds.

Entry	Substrate	Ligand	Activated C–H	Tertiary C–H	A : T
			60	61	62
1		tBuipy	20%	55%	1 : 2.8
2		tpa	59%	25%	2.4 : 1
3		tBuipy	21%	54%	1 : 2.6
4		tpa	63%	—	>20 : 1
5		tBuipy	11%	69%	1 : 6.3
6		tpa	42%	54%	1 : 1.3
7		tBuipy	28%	30%	1 : 1.1
8		tpa	74%	8%	9.3 : 1
9		tBuipy	21%	51%	1 : 2.4
10		tpa	37%	26%	1.4 : 1

These initial empirical results provided key insights for ligand design to further the scope of site-selective C–N bond formations. Attractive noncovalent interactions (NCIs), including aromatic  $\pi$ ... $\pi$  and metal... $\pi$  interactions, are well-known to direct reactivity in biochemical reactions and have been leveraged to control selectivity in synthetic organic chemistry.<sup>44,45</sup> The Schomaker group highlighted the role of NCIs in site-selective, silver-catalyzed nitrene transfer (Table 5)<sup>46</sup> and found that the preference for amination of an electron-rich tertiary alkyl C(sp<sup>3</sup>)–H bond can be overridden in favor of benzylic C–H amination by using a AgOTf catalyst supported by a tpa ligand (Table 5, Entries 1–2, 4–5, 7–8). Notably, modulating the steric environment of the tpa ligand by installing an *ortho* methyl substituent on the pyridine rings resulted in a switch in the site-selectivity (Table 5, Entry 3). Variable temperature (VT) NMR studies suggested this was due to a change in the coordination environment of the silver complex, where the (*o*-Me)tpa ligand favors a dimeric structure in solution. However, increasing the electron density of the pyridines on the tpa ligand by installing a *para* dimethylamino group

(Table 5, Entry 6) improved the selectivity for amination of an electron-poor C–H as compared to the parent tpa ligand.

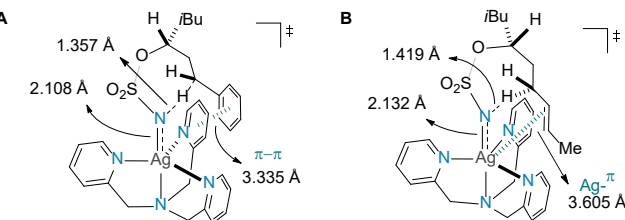
**Table 5.** Experimental evidence suggesting NCIs play a key role in selective nitrene transfer into benzylic C–H bonds.

	AgOTf ligand PhIO Solvent, Temp.		
Entry	Substrate	Ligand	Activated C–H Tertiary C–H A : T
1		tpa <sup>a</sup>	56% 20% 2.8 : 1
2		tpa <sup>b</sup>	73% 17% 4.3 : 1
3		( <i>o</i> -Me)tpa <sup>a</sup>	23% 49% 1 : 2.1
4		tpa <sup>a</sup>	57% 31% 1.8 : 1
5		tpa <sup>b</sup>	65% 18% 3.6 : 1
6		( <i>p</i> -Me <sub>2</sub> N) <sub>3</sub> tpa <sup>c</sup>	71% 10% 7.1 : 1
7		tpa <sup>a</sup>	70% 15% 4.7 : 1
8		tpa <sup>b</sup>	84% — >20 : 1

<sup>a</sup>CH<sub>2</sub>Cl<sub>2</sub>, rt; <sup>b</sup>CHCl<sub>3</sub>, -20 °C; <sup>c</sup>CH<sub>2</sub>Cl<sub>2</sub>, -20 °C

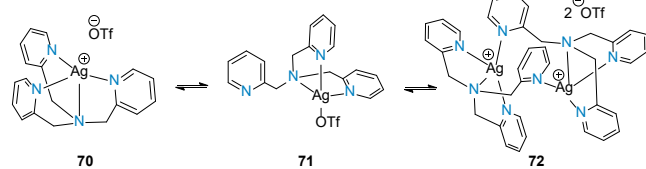
Although the examples in Table 5 provide indirect evidence for the role of NCIs in silver-catalyzed NT, detailed computations provided further support for the presence of directing, attractive noncovalent  $\pi$ ... $\pi$  interactions (NCIs, Scheme 9). Computational analyses revealed that the lowest energy active species can be formulated as an Ag(II)-nitrene radical anion. Importantly, the calculated transition states showed attractive  $\pi$ ... $\pi$  interactions between the aryl moiety of the substrate and the pyridine arm of the tpa ligand **14**, supporting the hypothesis that NCIs are at least partially responsible for the preference for amination of the benzylic C–H bond.<sup>47–49</sup> According to computational studies, an olefin-containing substrate (Scheme 9B) exhibited a Ag... $\pi$  interaction in the transition state, which explained the high chemo- and site-selectivity for allylic C–H amination (>19:1 site-selectivity) over competing aziridination or insertion into the tertiary alkyl C(sp<sup>3</sup>)–H bond.

**Scheme 9.** Computational studies of NCIs between tpa-supported silver complexes and substrates with competing reactive C–H bonds.



Variable temperature (VT) and DOSY NMR studies of (tpa)AgOTf in solution showed two different fluxional modes: 1) rapid association/dissociation of one arm of the tpa ligand to silver (Scheme 10, **70**  $\rightleftharpoons$  **71**) and 2) an equilibrium between monomeric and dimeric species (Scheme 10, **71**  $\rightleftharpoons$  **72**).<sup>50</sup> Based on these spectroscopic analyses, it was hypothesized reducing the fluxionality of the silver complex could improve the site-selectivity of NT.

**Scheme 10.** Dynamic nature of the (tpa)AgOTf complex.



Based on this hypothesis, the Schomaker group prepared new Ag complexes supported by the multidentate nitrogenated ligands  $[(\text{Py}_5\text{Me}_2)\text{AgOTf}]_2$  and  $(\alpha\text{-Me})\text{-anti-Py}_3\text{PipAgOTf}$  (Figure 3).<sup>51,52</sup>

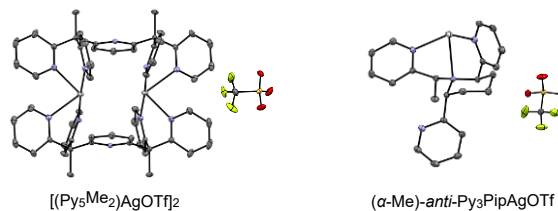


**Figure 3.** X-ray structures of  $[(\text{Py}_5\text{Me}_2)\text{AgOTf}]_2$  and  $(\alpha\text{-Me})\text{-anti-Py}_3\text{PipAgOTf}$ .

Similar to tpa **14**, Ag complexes formed using  $\text{Py}_5\text{Me}_2$  **16** and  $(\alpha\text{-Me})\text{-anti-Py}_3\text{Pip}$  **17** preferred C–N bond formation at benzylic, allylic and propargylic C–H bonds over unactivated  $\text{C}(\text{sp}^3)\text{-H}$  bonds (Table 6). Improved selectivity was attributed to the greatly decreased fluxionality of these complexes, as well as potential enhancements in directing NCIs between the substrate and the catalyst.

**Table 6.** Enhanced regioselectivity for activated C–H bonds.

Entry	Substrate	Ligand	Activated C–H		
			Tertiary C–H	A : T	
1		$\text{Py}_2\text{Me}_5^a$	58%	22%	<b>2.6 : 1</b>
2		$\alpha\text{-Me-anti-Py}_3\text{Pip}^b$	74%	12%	<b>6.1 : 1</b>
3		tpa <sup>b</sup>	73%	17%	<b>4.3 : 1</b>
4		$\text{Py}_2\text{Me}_5^a$	66%	—	<b>&gt;20 : 1</b>
5		$\alpha\text{-Me-anti-Py}_3\text{Pip}^b$	82%	—	<b>&gt;20 : 1</b>
6		tpa <sup>b</sup>	94%	5%	<b>19 : 1</b>
7		$\text{Py}_2\text{Me}_5^a$	60%	7%	<b>8.5 : 1</b>
8		$\alpha\text{-Me-anti-Py}_3\text{Pip}^b$	46%	11%	<b>4.2 : 1</b>
9		tpa <sup>b</sup>	52%	17%	<b>3.1 : 1</b>

<sup>a</sup> $\text{CH}_2\text{Cl}_2$ , rt; <sup>b</sup> $\text{CHCl}_3$ , -20 °C

### 3.1.2 Cyclic Tertiary $\text{C}(\text{sp}^3)\text{-H}$ Bonds vs. Acyclic Tertiary $\text{C}(\text{sp}^3)\text{-H}$ Bonds

Compared to selecting between two very different C–H bonds, achieving selectivity between two similar tertiary  $\text{C}(\text{sp}^3)\text{-H}$  sites is a greater challenge. However, the ability to tune the steric environments of diverse silver coordination complexes through judicious selection of ligands enabled selective C–H amination between these similar C–H bonds. A low-coordinate silver complex,  $(\text{Me}_4\text{phen})\text{AgOTf}$ , preferentially formed **77**, with increased selectivity as the ring size was increased, perhaps due to greater rates of *pseudo*-equatorial C–H bond oxidation (Table 7, Entries 1, 3 and 5).<sup>53</sup> In contrast, use of  $\text{Py}_5\text{Me}_2$  **16** as the ligand increased the preference for formation of **78**, although a complete reversal of selectivity was only obtained in a substrate bearing a cHex group as the competing functionality (Table 7, Entries 2, 4, and 6). Additional work is needed to better understand the subtle factors that influence the outcomes in this challenging site-selective NT.

**Table 7.** Regioselective C–H amination between two tertiary  $\text{C}(\text{sp}^3)\text{-H}$  bonds.

Entry	Substrate	Ligand	Cyclic C–H	Acyclic C–H	Cy : Acy
1		Me4phen	66%	26%	<b>2.5 : 1</b>
2		$\text{Py}_5\text{Me}_2$	56%	31%	<b>1.8 : 1</b>
3		Me4phen	79%	16%	<b>5.0 : 1</b>
4		$\text{Py}_5\text{Me}_2$	20%	77%	<b>1 : 3.9</b>
5		Me4phen	84%	12%	<b>7.3 : 1</b>
6		$\text{Py}_5\text{Me}_2$	54%	42%	<b>1.3 : 1</b>

### 3.1.3 Five-Membered versus Six-Membered Heterocycle Formation

Despite the ability of silver-catalyzed intramolecular site-selective NT to discriminate between certain types of competing C–H bonds to form products of the same ring size, the ability to access rings of differing sizes in a predictable manner is more challenging.<sup>54</sup> The design of sterically-differentiated Ag complexes that can control the approach of the nitrene to a given C–H bond enabled the formation of either 5- or 6-membered heterocycles from simple sulfonamide-bearing precursors.

Substrate **79**, which contains both benzylic and homobenzylic C–H bonds, was employed for silver-catalyzed amination either using  $\text{Py}_5\text{Me}_2$  **16** or  $t\text{Bu}_3\text{tpy}$  **13** as a ligand (Table 8).<sup>54</sup> Utilizing  $[(\text{Py}_5\text{Me}_2)\text{AgOTf}]_2$  resulted

in preferred insertion at the benzylic position to form the five-membered sultam, while  $[(t\text{Bu}_3\text{tpy})\text{AgOTf}]_2$  favored formation of the six-membered sultam. Interestingly, an increasing amount of benzylic amination was observed with  $\text{Py}_5\text{Me}_2$  **16** when the steric bulk was increased at the  $\zeta$ -carbon, suggesting the sterics of the catalyst are likely the key factor in selectivity.

**Table 8.** Regioselective C–H amination forming 5- and 6-membered heterocycles.

Entry	Substrate	Ligand	$\delta$ -C–H	$\epsilon$ -C–H	$\delta : \epsilon$
1		$\text{Py}_5\text{Me}_2$	49%	30%	
2		$t\text{Bu}_3\text{tpy}$	11%	65%	
3		$\text{Py}_5\text{Me}_2$	76%	12%	
4		$t\text{Bu}_3\text{tpy}$	18%	68%	
5		$\text{Py}_5\text{Me}_2$	46%	10%	
6		$t\text{Bu}_3\text{tpy}$	12%	72%	
<i>R</i> = adamantyl					

A (–)-menthol derivative **83** bearing two competing tertiary  $(\text{sp}^3)$ -H bonds was also examined for control over ring size in the amination event.<sup>55,56</sup> The use of a dmBOX ligand, which generates a monomeric silver complex, favored the formation of a six-membered heterocycle (Table 9, Entry 1). In contrast, a  $[(\text{Py}_5\text{Me}_2)\text{Ag}(\text{ClO}_4)]_2$  catalyst, which is dimeric in solution and sterically congested, resulted in excellent selectivity for reaction at the  $\delta$ -site (Table 9, Entry 5).

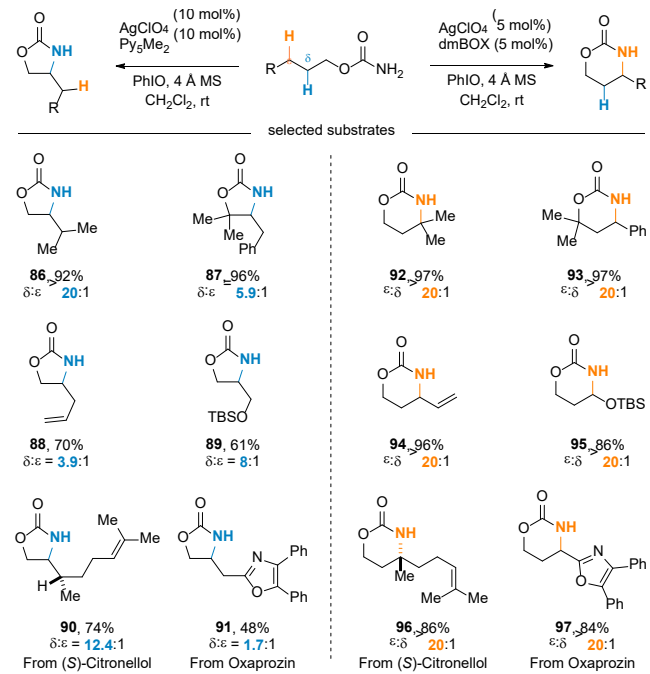
**Table 9.** Silver catalysts for tunable amidations of  $\delta$ - and  $\epsilon$ -C–H bonds.

Entry	Ligand	$\delta$ -C–H	$\epsilon$ -C–H	$\delta : \epsilon$
1	dmBOX	15%	84%	
2	$\text{Me}_4\text{phen}$	19%	73%	
3	tpa	73%	18%	
4	$t\text{Bu}_3\text{tpy}$	71%	17%	
5	$\text{Py}_5\text{Me}_2$	84%	–	

The scope of the reaction to furnish either five- or six-membered cyclic carbamates was found to give good-to-

excellent product ratios (Scheme 11). In particular, the  $[(\text{Py}_5\text{Me}_2)\text{Ag}(\text{ClO}_4)]_2$  catalyst showed moderate-to-good selectivity for unactivated C–H bonds even in the presence of weaker benzylic and allylic C–H bonds. Furthermore, the versatility of the developed method was highlighted by late-stage C–H aminations of biologically relevant compounds.

**Scheme 11.** Representative examples of tunable, silver-catalyzed heterocycle formation.



KIE experiments for both catalysts revealed essentially no differences in KIE values, indicating that the mechanisms of both pathways are likely similar and proceed via either a concerted or HAT mechanism, followed by rapid radical recombination. Linear free-energy relationships (LFER) using Charton's modified Taft equation showed that the coordination geometries of ligands on silver are the key to achieving excellent site-selectivity. DFT studies on the monomeric (dmBOX) $\text{AgClO}_4$  showed a near-linear  $\text{N}\cdots\text{H}\cdots\text{C}$  geometry favoring a 7-membered transition state, while the dimeric silver complex with  $\text{Py}_5\text{Me}_2$  presents a congested binding pocket which favors the 6-membered ring transition state (Figure 4).

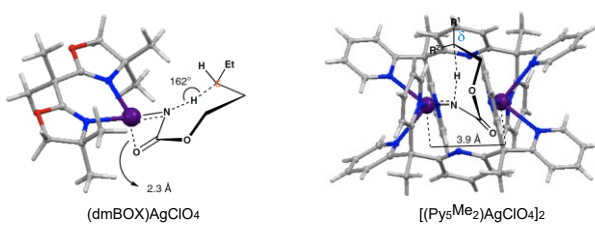


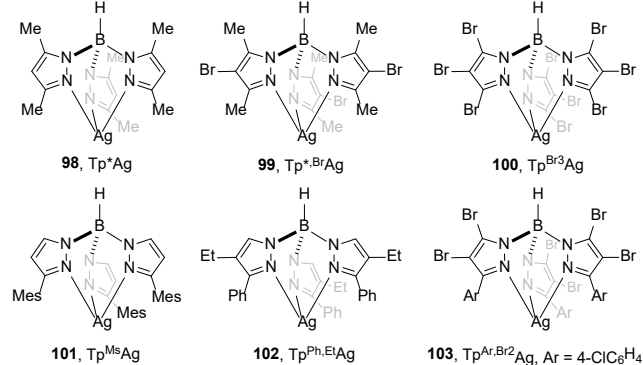
**Figure 4.** Steric control of regioselective C–H amidation. Copyright © 2019, under exclusive license to Springer Nature Limited.

### 3.2 Intermolecular Regioselective Nitrene Transfer

#### 3.2.1 Intermolecular Regioselective C–H Amination

Silver-catalyzed C–H amination chemistry has historically been dominated by nitrogenated bidentate ligands. However, Dias's seminal studies on scorpionate ligands with silver showcased the potential of tridentate ligands in silver-catalyzed site-selective C–H functionalization.<sup>57</sup> The development of well-defined silver-scorpionate complexes (**98–103**) as candidates for C–H amination reactions is a promising approach for extending the utility of silver catalysis (Scheme 12).

**Scheme 12.** Diverse silver-scorpionate complexes.



In 2008, Pérez and coworkers developed C–H amidations catalyzed by silver-scorpionate complexes (Table 10).<sup>58</sup> In this study, linear or branched hydrocarbons were functionalized in a site-selective manner.

**Table 10.** Ag-scorpionate-catalyzed intermolecular regioselective C–H amination of alkanes.

A		[Ag] PhI=N-Ts			
Entry	[Ag]	1° C–H	2° C–H	2° C–H	1° : 2° : 2°
1	Tp*Ag, <b>98</b>	3%	23%	14%	1 : 8.3 : 5
2	Tp*BrAg, <b>99</b>	7%	38%	20%	1 : 6 : 3
3	TpMsAg, <b>101</b>	6%	21%	13%	1 : 3.5 : 2

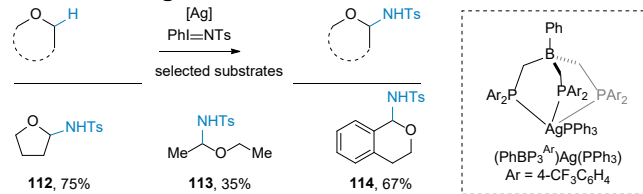
B		[Ag] PhI=N-Ts			
Entry	[Ag]	1° C–H	2° C–H	3° C–H	1° : 2° : 3°
1	Tp*Ag, <b>98</b>	—	4%	36%	0 : 1 : 9
2	Tp*BrAg, <b>99</b>	—	8%	72%	0 : 1 : 9
3	TpMsAg, <b>101</b>	—	4%	11%	0 : 1 : 2.8

It was shown that the silver-scorpionate catalysts preferred to amine secondary C–H over primary C–H bonds, but tertiary C–H bonds were the most highly favored. This suggests that electronics is the primary determinant of selectivity in Ag-scorpionate-catalyzed C–H amidations.<sup>59</sup> In

addition, the Tp\*BrAg complex **99** was the most active when compared to other well-defined silver complexes.

In 2014, Pérez and coworkers developed a new type of silver complex, where a fluorinated trisphosphinoborate ligand coordinates to the silver, enabling nitrene transfer reactions at ethereal C(sp<sup>3</sup>)–H bonds (Scheme 13).<sup>60</sup> Later, Crabtree and Gunnoe described a metal-free condition for a similar transformation of ethereal C–H to C–N bonds in the presence of a hypervalent iodine oxidant.<sup>61</sup>

**Scheme 13.** Ag-nitrene insertion into ethereal C–H bonds.



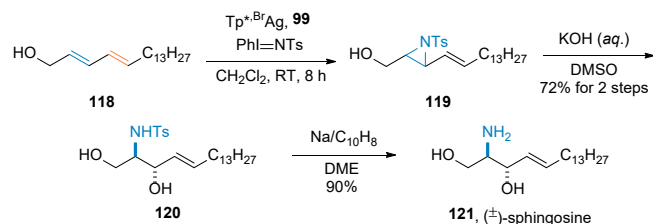
#### 3.2.2 Intermolecular Regioselective Aziridination

In 2010, Pérez and coworkers reported regioselective aziridinations of conjugated dienes in a highly stereoselective fashion (Table 11).<sup>62,63</sup> High regioselectivity was attributed to a directing effect of the hydroxy group (Table 11, Entries 1, 3, 4). If the hydroxy group was protected, lower conversion was noted, along with a substantial decrease in the regioselectivity (Table 11, Entry 2). An “asynchronous concerted” mechanism was later revealed by detailed computational studies, where the initial metallonitrene is considered to be a biradical species, as opposed to the usual singlet species. The utility of this chemistry was demonstrated in the synthesis of a racemic form of sphingosine **121** in a regio- and stereoselective aziridination manner (Scheme 14).

**Table 11.** Ag-scorpionate-catalyzed intermolecular regioselective aziridination of conjugated dienes.

		Tp*BrAg, <b>99</b> PhI=N-Ts		Regioselectivity	
Entry	R, R <sup>1</sup>	alkoxy C=C	alkyl C=C	trans : cis	
1	H, Me	90%	10%	9 : 1	>98 : 2
2	Bn, Me	40%	26%	1.5 : 1	98 : 2
3	H, H	88%	12%	9 : 1	>98 : 2
4	H, Ph	93%	7%	13.3 : 1	>98 : 2

**Scheme 14.** Synthesis of (±)-sphingosine.



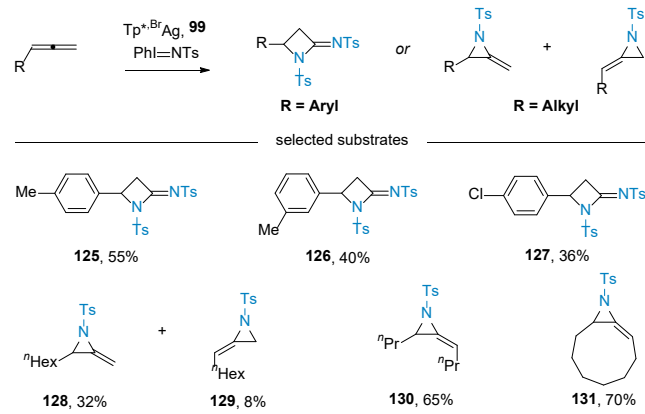
Further investigations from the Pérez group showed different site-selectivity when unconjugated dienes were employed (Table 12, Entry 1).<sup>63</sup> In sharp contrast, protection of the alcohol as an acetate group led to a dramatic change in regioselectivity, where the aziridine **124** was formed as the major product (Table 12, Entry 2).

**Table 12.** Ag-scorpionate-catalyzed intermolecular regioselective aziridination of unconjugated dienes.

Entry	R	alcoxy C=C	alkyl C=C	Regioselectivity
		50%	41%	1.2 : 1
2	Ac	10%	83%	1 : 8.3

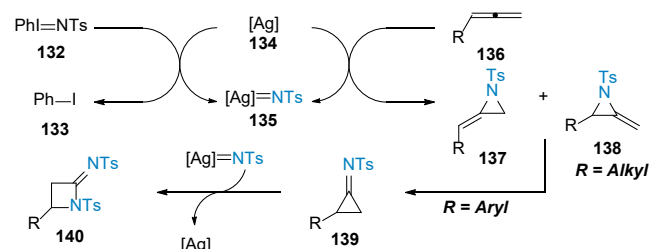
More recently, the Pérez group successfully developed intermolecular allene functionalizations by using a silver-scorpionate catalyst (Scheme 15).<sup>64</sup> Differentially substituted allenes provided either azetidine or methylene aziridine derivative as products.

**Scheme 15.** Ag-scorpionate-catalyzed NT to aryl allenes.



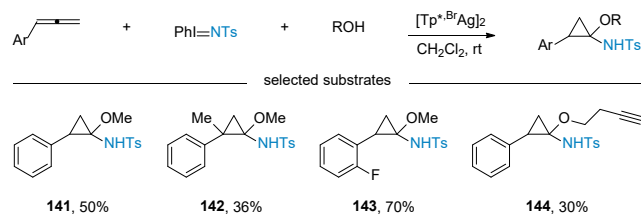
Computational studies led to a detailed understanding of how silver is able to catalyze the formation of the four-membered heterocycle via a key cyclopropanimine intermediate **139** (Scheme 16).

**Scheme 16.** Proposed mechanism for NT to allenes catalyzed by  $[Tp^*BrAg]_2$  **134**.



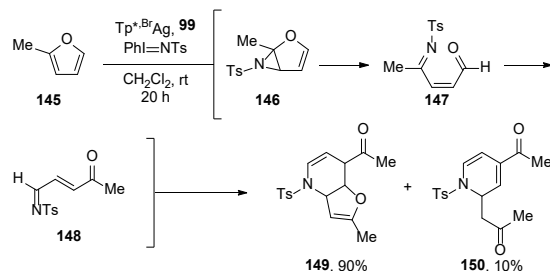
It is noteworthy that computational insights were further corroborated through reactions employing alcohols as an additional coupling partner to afford aminocyclopropanol derivatives (Scheme 17).

**Scheme 17.** Experimental evidence for intermediate **139**.



Finally, the Pérez group also reported a transformation of 2-methylfuran **145** to 1,2-dihydropyridine **150** by silver-scorpionate-induced tandem catalysis (Scheme 18).<sup>65</sup>

**Scheme 18.** Selective transformation of furan by silver-induced concurrent tandem catalysis.

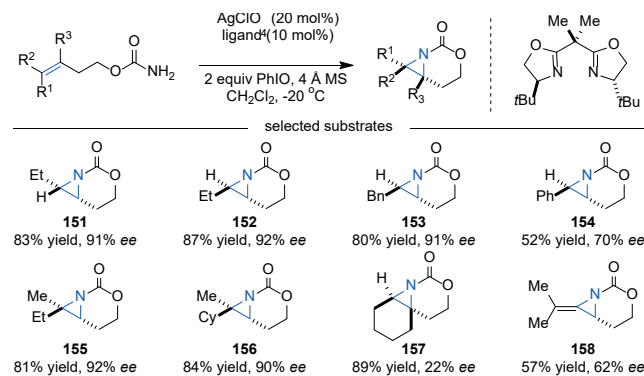


#### 4 Enantioselective Nitrene Transfer

##### 4.1 Enantioselective Aziridination

Transition metal-catalyzed asymmetric NT transforms simple nitrene precursors into enantioenriched amines. Enantioselective aziridinations have been achieved with copper,<sup>66–68</sup> rhodium,<sup>69</sup> ruthenium,<sup>17–19</sup> and cobalt<sup>70</sup>, albeit with limited substrate scope (styrenes, terminal olefins). In 2017, the Schomaker group disclosed the first examples of silver-catalyzed chemo- and enantioselective intramolecular aziridination (Scheme 19).<sup>71</sup>

**Scheme 19.** Selected scope for asymmetric aziridination.



In this study, the combination of a silver salt with a chiral BOX ligand provided not only excellent chemoselectivity, also good enantiomeric excess. A variety of 1,2-substituted (151–154) and 1,1',2-substituted homoallylic carbamates (155–156) were compatible with this process, affording the corresponding aziridines in good yield and *ee*. Minor amounts of the competing C–H were noted, but were not isolated, as the focus was on the *ee* of the aziridine product. The 1,2,2'-substituted alkene 157 and allene 158 were also successful, albeit with reduced *ee*. A model for stereochemical induction was proposed based on the absolute stereochemistry of 153 and the *ee* of products bearing various alkene substitution patterns (Figure 5). The poor *ee* observed in substrate 157 is proposed to result from undesired steric interactions between substitution at  $R^3$  and the catalyst.

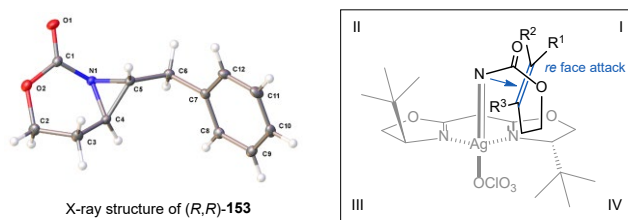


**Figure 5.** Stereochemical model for asymmetric aziridination. Copyright © 2017, John Wiley and Sons.

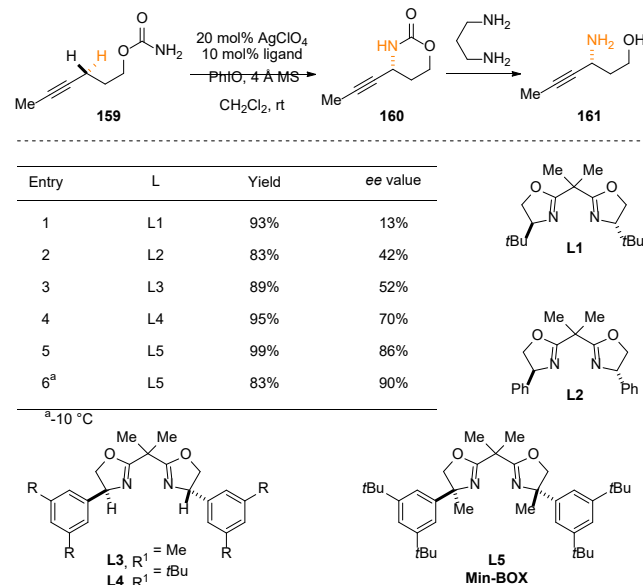
#### 4.2 Enantioselective C–H Amination

Enantioenriched  $\gamma$ -amino alcohols are key structural motifs in biorelevant compounds and also serve as chiral ligands. Asymmetric amination of primarily benzylic C–H bonds via NT has been studied with ruthenium<sup>72</sup> and rhodium<sup>73</sup> to access  $\gamma$ -amino alcohols. In 2020, the Schomaker group was able to achieve the first examples of enantioselective silver-catalyzed propargylic C–H aminations to afford enantioenriched  $\gamma$ -alkynyl  $\gamma$ -amino alcohol products.<sup>74</sup>

A survey of common bis(oxazoline) (BOX) ligand scaffolds revealed that aryl-BOX ligands were the optimal framework for optimization. No competing reaction at the alkene was noted and the mass balance consisted only of remaining alkyne. Interestingly, both increasing the sterics of the aryl groups and rendering the chiral center a quaternary carbon (Min-BOX) greatly improved the enantioselectivity (Table 13). VT NMR studies and DFT calculations on the Min-BOX and similar model substrates revealed that the silver complex in solution exists as a monomeric species and suggest that placing a methyl group at the chiral center decreases the rotational barrier around the aryl-oxazoline C–C bond. This may enforce a more rigid conformation of the catalyst in the enantiodetermining transition state.

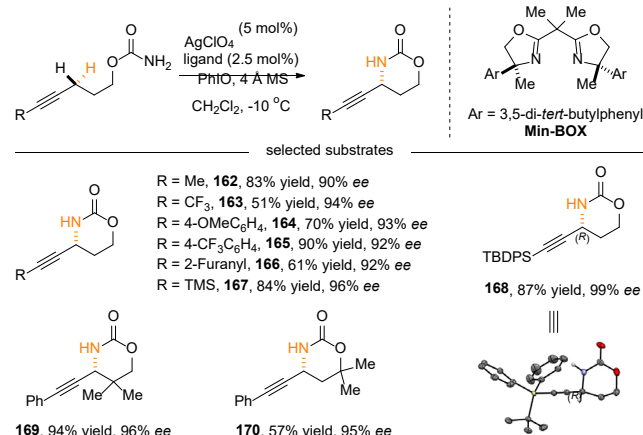
These robust conditions were showcased using several different carbamates (Scheme 20). Substrates containing alkyl (162–163), aryl (164–165), heteroaryl (166) and silyl (167–168) substitutions at the distal alkyne carbon were fully tolerated, regardless of the steric and electronic modifications, as in 169–170. A comparable mechanism to

**Table 13.** Silver-catalyzed asymmetric C–H amination.



to previous reports<sup>41,42,46</sup> was proposed based on experimental and computational studies (Scheme 21). Importantly, the enantiodetermining step was calculated to be the H-atom transfer (HAT) step, with **TS-(R)** 1.7 kcal/mol lower in energy than **TS-(S)**.

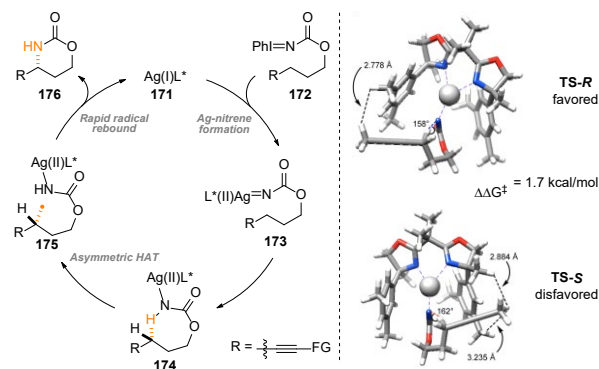
**Scheme 20.** Representative scope for asymmetric amination of propargylic C–H bonds.



#### 5 Conclusion and Future Perspectives

During the last decade, transition metal-catalyzed nitrene transfer has experienced a rapid growth. In particular, the recent progress of silver-catalyzed nitrene transfer reactions have clearly illustrated the unique features of silver in C–N bond forming reactions. Notably, a careful selection and modification of ligand scaffold have played a pivotal role in controlling both reactivity and selectivity. Spectroscopic and crystallographic analyses helped to gain an insight of catalyst's dynamic behavior while computational studies deciphered experimental findings.

**Scheme 21.** Proposed mechanism of Ag-catalyzed enantioselective propargylic C–H amination.



and outlined reaction mechanisms. Indeed, these achievements of chemo-, regio-, and enantioselective nitrene transfer with silver catalysts set the stage for further improvement in the future.

Despite this progress, there are still many challenges to be met using Ag-catalyzed nitrene transfer. For example, while silver complexes supported by *(S,S)*-Min-BOX give good *ee* for aminations of propargylic and benzylic C–H bonds, further catalyst design aided by computational studies is required to expand the scope to amination of allylic and unactivated methylene C–H bonds. A broader range of chiral supporting ligands for silver salts are also likely to yield promising leads for both intra- and intermolecular asymmetric amination reactions.

Another challenge is to design catalysts that are able to override the inherent preference for amination at a more electron-rich or ‘activated’ C–H bond over an electron-deficient C–H bonds. In this context, ligand designs that facilitate  $\pi$ – $\pi$  or Ag– $\pi$  interactions between the catalyst and the substrate, as informed by computational studies, are a productive avenue for further investigations.<sup>46</sup> Similarly, catalysts that can engage non-covalent interactions between the catalyst and substrate may be able to achieve tunable, selective aminations of competing benzylic C–H bonds or choose between amination of allylic *vs.* benzylic, benzylic *vs.* propargylic or allylic *vs.* propargylic C–H bonds.

A recent report from the Schomaker and Liu groups shows that the nature of the nitrene precursor can also exert a big impact on the outcome of the nitrene transfer reaction.<sup>56</sup> Further investigations into a broader range of nitrene precursor/catalyst combinations are likely to reveal interesting trends and other strategies to tune chemo-, site- and enantioselectivity. These insights can be extended to achieve ligand-controlled, intermolecular site- and enantioselective aminations of C–H bonds, a long-standing challenge in the field that has not yet been solved.

Finally, the ability to employ a wide range of ligands for Ag-catalyzed NT bodes well for efforts directed towards catalysts capable of the selective functionalization of primary C–H bonds. Manipulating the steric environment of the dimeric pocket of  $[(\text{Py}_5\text{Me}_2)\text{Ag}(\text{ClO}_4)]_2$ , coupled with the appropriate nitrene precursor, may unlock this useful

reactivity. Ultimately, we hope the community continues to build on this suite of silver catalysts capable of predictable and tunable chemo-, site-, and enantioselective aminations of C–H and C=C bonds. These catalysts can complement the toolbox of other reported transition metal catalysts to help revolutionize the way in which chemists approach the synthesis of valuable amines and late-stage functionalization of natural products and pharmaceuticals.

## AUTHOR INFORMATION

### Corresponding Author

**\*Jennifer M. Schomaker** – Department of Chemistry, Madison, Wisconsin 53706, United States; [orcid.org/0000-0003-1329-950X](http://orcid.org/0000-0003-1329-950X); Email: [schomakerj@chem.wisc.edu](mailto:schomakerj@chem.wisc.edu)

### Authors

**Wentan Liu** – Department of Chemistry, Madison, Wisconsin 53706, United States; [orcid.org/0000-0002-8762-489X](http://orcid.org/0000-0002-8762-489X)

**Isaac Choi** – Department of Chemistry, Madison, Wisconsin 53706, United States; [orcid.org/0000-0002-9207-4845](http://orcid.org/0000-0002-9207-4845)

**Emily E. Zerull** – Department of Chemistry, Madison, Wisconsin 53706, United States; [orcid.org/0000-0003-1339-1859](http://orcid.org/0000-0003-1339-1859)

### Author Contributions

<sup>†</sup>These authors contributed equally to this manuscript.

The manuscript was written through contributions of all authors. All authors have given approval to the final version of the manuscript.

### Funding Sources

J.M.S. and the Schomaker group are grateful to the NSF for funding through awards 1664374 and 1954325 to support the research highlighted in this perspective.

### Notes

The authors declare no competing financial interest.

### ACKNOWLEDGMENT

Dr. Charlie Fry and Dr. Heike Hofstetter of the University of Wisconsin-Madison are thanked for assistance with NMR spectroscopy, while Dr. Martha Vestling of UW-Madison is thanked for her assistance with collecting MS data.

### REFERENCES

1. Muller, P.; Fruit, C., Enantioselective catalytic aziridinations and asymmetric nitrene insertions into CH bonds. *Chem. Rev.* **2003**, *103*, 2905–2920.
2. Driver, T. G., Recent advances in transition metal-catalyzed *N*-atom transfer reactions of azides. *Org. Biomol. Chem.* **2010**, *8*, 3831–3846.
3. Chang, J. W. W.; Ton, T. M. U.; Chan, P. W. H., Transition-metal-catalyzed aminations and aziridinations of C–H and C–C bonds with iminoiodinanes. *Chem. Rec.* **2011**, *11*, 331–357.
4. Lu, H.; Zhang, X. P., Catalytic C–H functionalization by metalloporphyrins: recent developments and future directions. *Chem. Soc. Rev.* **2011**, *40*, 1899–1909.

5. Dequierez, G.; Pons, V.; Dauban, P., Nitrene Chemistry in Organic Synthesis: Still in Its Infancy? *Angew. Chem., Int. Ed.* **2012**, *51*, 7384-7395.

6. Gephart, R. T.; Warren, T. H., Copper-Catalyzed  $sp^3$  C-H Amination. *Organometallics* **2012**, *31*, 7728-7752.

7. Roizen, J. L.; Harvey, M. E.; Du Bois, J., Metal-Catalyzed Nitrogen-Atom Transfer Methods for the Oxidation of Aliphatic C-H Bonds. *Acc. Chem. Res.* **2012**, *45*, 911-922.

8. Alderson, J. M.; Corbin, J. R.; Schomaker, J. M., Tunable, Chemo- and Site-Selective Nitrene Transfer Reactions through the Rational Design of Silver(I) Catalysts. *Acc. Chem. Res.* **2017**, *50*, 2147-2158.

9. Park, Y.; Kim, Y.; Chang, S., Transition Metal-Catalyzed C-H Amination: Scope, Mechanism, and Applications. *Chem. Rev.* **2017**, *117*, 9247-9301.

10. Chu, J. C. K.; Rovis, T., Complementary Strategies for Directed  $sp^3$  C-H Functionalization: A Comparison of Transition-Metal-Catalyzed Activation, Hydrogen Atom Transfer, and Carbene/Nitrene Transfer. *Angew. Chem., Int. Ed.* **2018**, *57*, 62-101.

11. Liu, Y.; You, T.; Wang, H.-X.; Tang, Z.; Zhou, C.-Y.; Che, C.-M., Iron- and cobalt-catalyzed  $C(sp^3)$ -H bond functionalization reactions and their application in organic synthesis. *Chem. Soc. Rev.* **2020**, *49*, 5310-5358.

12. Ju, M.; Schomaker, J. M., Nitrene transfer catalysts for enantioselective C-N bond formation. *Nat. Rev. Chem.* **2021**, *5*, 580-594.

13. Rodriguez, M. R.; Diaz-Requejo, M. M.; Pérez, P. J., Development of Molecular Complexity through Nitrene-Transfer Reactions Catalyzed by Copper and Silver Scorpionate Complexes. *Synlett* **2021**, *32*, 763-774.

14. Vine, L. E.; Zerull, E. E.; Schomaker, J. M., Taming Nitrene Reactivity with Silver Catalysts. *Synlett* **2021**, *32*, 30-44.

15. Kwart, H.; Khan, A. A., Copper-catalyzed decomposition of benzenesulfonyl azide cyclohexene solution. *J. Am. Chem. Soc.* **1967**, *89*, 1951-1953.

16. For selected references, see: a) Espino, C. G.; Fiori, K. W.; Kim, M.; Du Bois, J., Expanding the Scope of C-H Amination through Catalyst Design. *J. Am. Chem. Soc.* **2004**, *126*, 15378-15379. b)

17. Omura, K.; Murakami, M.; Uchida, T.; Irie, R.; Katsuki, T., Enantioselective aziridination and amination using *p*-toluenesulfonyl azide in the presence of Ru(salen)(CO) complex. *Chem. Lett.* **2003**, *32*, 354-355.

18. Omura, K.; Uchida, T.; Irie, R.; Katsuki, T., Design of a robust Ru(salen) complex: aziridination with improved turnover number using *N*-arylsulfonyl azides as precursors. *Chem. Commun.* **2004**, 2060-2061.

19. Kawabata, H.; Omura, K.; Uchida, T.; Katsuki, T., Construction of robust ruthenium(salen)(CO) complexes and asymmetric aziridination with nitrene precursors in the form of azide compounds that bear easily removable *N*-sulfonyl groups. *Chem. - Asian J.* **2007**, *2*, 248-256.

20. Hong, S. Y.; Park, Y.; Hwang, Y.; Kim, Y. B.; Baik, M.-H.; Chang, S., Selective formation of  $\gamma$ -lactams via C-H amidation enabled by tailored iridium catalysts. *Science* **2018**, *359*, 1016-1021.

21. Wang, H.; Park, Y.; Bai, Z.; Chang, S.; He, G.; Chen, G., Iridium-Catalyzed Enantioselective  $C(sp^3)$ -H Amidation Controlled by Attractive Noncovalent Interactions. *J. Am. Chem. Soc.* **2019**, *141*, 7194-7201.

22. Fantauzzi, S.; Caselli, A.; Gallo, E., Nitrene transfer reactions mediated by metallo-porphyrin complexes. *Dalton Trans.* **2009**, *28*, 5434-5443.

23. Lu, H.; Jiang, H.; Hu, Y.; Wojtas, L.; Zhang, X. P., Chemoselective intramolecular allylic C-H amination versus C=C aziridination through Co(II)-based metalloradical catalysis. *Chem. Sci.* **2011**, *2*, 2361-2366.

24. Lyaskovskyy, V.; Suarez, A. I. O.; Lu, H.; Jiang, H.; Zhang, X. P.; de Bruin, B., Mechanism of Cobalt(II) Porphyrin-Catalyzed C-H Amination with Organic Azides: Radical Nature and H-Atom Abstraction Ability of the Key Cobalt(III)-Nitrene Intermediates. *J. Am. Chem. Soc.* **2011**, *133*, 12264-12273.

25. Paradine, S. M.; White, M. C., Iron-Catalyzed Intramolecular Allylic C-H Amination. *J. Am. Chem. Soc.* **2012**, *134*, 2036-2039.

26. Lu, H.; Li, C.; Jiang, H.; Lizardi, C. L.; Zhang, X. P., Chemoselective amination of propargylic  $C(sp^3)$ -H bonds by cobalt(II)-based metalloradical catalysis. *Angew. Chem., Int. Ed.* **2014**, *53*, 7028-7032.

27. Paradine, S. M.; Griffin, J. R.; Zhao, J.; Petronico, A. L.; Miller, S. M.; Christina White, M., A manganese catalyst for highly reactive yet chemoselective intramolecular  $C(sp^3)$ -H amination. *Nat. Chem.* **2015**, *7*, 987-994.

28. Clark, J. R.; Feng, K.; Sookezian, A.; White, M. C., Manganese-catalysed benzyllic  $C(sp^3)$ -H amination for late-stage functionalization. *Nat. Chem.* **2018**, *10*, 583-591.

29. Cui, Y.; He, C., Efficient Aziridination of Olefins Catalyzed by a Unique Disilver(I) Compound. *J. Am. Chem. Soc.* **2003**, *125*, 16202-16203.

30. Rigoli, J. W.; Weatherly, C. D.; Alderson, J. M.; Vo, B. T.; Schomaker, J. M., Tunable, Chemoselective Amination *via* Silver Catalysis. *J. Am. Chem. Soc.* **2013**, *135*, 17238-17241.

31. Levason, W.; Spicer, M. D., The chemistry of copper and silver in their higher oxidation states. *Coord. Chem. Rev.* **1987**, *76*, 45-120.

32. Leschke, M.; Rheinwald, G.; Lang, H., Bipy, phen, and  $P(C_6H_4CH_2NMe_2-2)_3$  in the synthesis of cationic silver(I) complexes. The solid-state structures of  $[P(C_6H_4CH_2NMe_2-2)_3]AgOTf$  and  $[Ag(phen)_2]OTf$ . *Z. Anorg. Allg. Chem.* **2002**, *628*, 2470-2477.

33. Du, J.-L.; Hu, T.-L.; Zhang, S.-M.; Zeng, Y.-F.; Bu, X.-H., Tuning silver(I) coordination architectures by ligands design: from dinuclear, trinuclear, to 1D and 3D frameworks. *CrystEngComm* **2008**, *10*, 1866-1874.

34. Hung-Low, F.; Renz, A.; Klausmeyer, K. K., An X-ray diffraction study of anion and ratio dependence in the formation of discrete molecules versus polymeric arrays involving silver salts and bipyridine ligands. *Polyhedron* **2009**, *28*, 407-415.

35. Hung-Low, F.; Renz, A.; Klausmeyer, K. K., X-ray Crystal Structures of Discrete and Polymeric Silver Based Molecules Containing 4,4'-Dimethyl-2,2'-Bipyridine and 2,2'-Bipyridine. *J. Chem. Crystallogr.* **2009**, *39*, 438-444.

36. Hung-Low, F.; Renz, A.; Klausmeyer, K. K., X-ray Crystal Structures of Silver Based Molecules Containing 5,5'-Dimethyl-2,2'-bipyridine and 2,2'-bipyridine. *J. Chem. Crystallogr.* **2011**, *41*, 1174-1179.

37. Zhang, H.-Y.; Chen, L.; Song, H.-B.; Zi, G.-F., Synthesis, structure, and catalytic activity of chiral silver(I) and copper(II) complexes with biaryl-based nitrogen-containing ligands. *Inorg. Chim. Acta* **2011**, *366*, 320-336.

38. Au, S.-M.; Huang, J.-S.; Yu, W.-Y.; Fung, W.-H.; Che, C.-M., Aziridination of Alkenes and Amidation of Alkanes by Bis(tosylimido)ruthenium(VII) Porphyrins. A Mechanistic Study. *J. Am. Chem. Soc.* **1999**, *121*, 9120-9132.

39. Au, S.-M.; Huang, J.-S.; Che, C.-M.; Yu, W.-Y., Amidation of Unfunctionalized Hydrocarbons Catalyzed by Ruthenium Cyclic Amine or Bipyridine Complexes. *J. Org. Chem.* **2000**, *65*, 7858-7864.

40. Leung, S. K.-Y.; Tsui, W.-M.; Huang, J.-S.; Che, C.-M.; Liang, J.-L.; Zhu, N., Imido Transfer from Bis(imido)ruthenium(VI) Porphyrins to Hydrocarbons: Effect of Imido Substituents, C-H Bond Dissociation Energies, and Ru<sup>VI/V</sup> Reduction Potentials. *J. Am. Chem. Soc.* **2005**, *127*, 16629-16640.

41. Weatherly, C.; Alderson, J. M.; Berry, J. F.; Hein, J. E.; Schomaker, J. M., Catalyst-controlled nitrene transfer by tuning metal:ligand ratios: insight into the mechanisms of chemoselectivity. *Organometallics* **2017**, *36*, 1649-1661.

42. Dolan, N. S.; Scamp, R. J.; Yang, T.; Berry, J. F.; Schomaker, J. M., Catalyst-Controlled and Tunable, Chemoselective Silver-Catalyzed

Intermolecular Nitrene Transfer: Experimental and Computational Studies. *J. Am. Chem. Soc.* **2016**, *138*, 14658-14667.

43. Alderson, J. M.; Phelps, A. M.; Scamp, R. J.; Dolan, N. S.; Schomaker, J. M., Ligand-Controlled, Tunable Silver-Catalyzed C-H Amination. *J. Am. Chem. Soc.* **2014**, *136*, 16720-16723.

44. Burley, S. K.; Petsko, G. A., Aromatic-aromatic interaction: a mechanism of protein structure stabilization. *Science* **1985**, *229*, 23-28.

45. Dougherty, D. A., Cation- $\pi$  interactions in chemistry and biology: a new view of benzene, Phe, Tyr, and Trp. *Science* **1996**, *271*, 163-168.

46. Huang, M.; Yang, T.; Paretsky, J. D.; Berry, J. F.; Schomaker, J. M., Inverting Steric Effects: Using "Attractive" Noncovalent Interactions To Direct Silver-Catalyzed Nitrene Transfer. *J. Am. Chem. Soc.* **2017**, *139*, 17376-17386.

47. Knowles, R. R.; Jacobsen, E. N., Attractive noncovalent interactions in asymmetric catalysis: Links between enzymes and small molecule catalysts. *Proc. Natl. Acad. Sci. U. S. A.* **2010**, *107*, 20678-20685.

48. Krenske, E. H.; Houk, K. N., Aromatic Interactions as Control Elements in Stereoselective Organic Reactions. *Acc. Chem. Res.* **2013**, *46*, 979-989.

49. Neel, A. J.; Hilton, M. J.; Sigman, M. S.; Toste, F. D., Exploiting non-covalent  $\pi$  interactions for catalyst design. *Nature* **2017**, *543*, 637-646.

50. Huang, M.; Corbin, J. R.; Dolan, N. S.; Fry, C. G.; Vinokur, A. I.; Guzei, I. A.; Schomaker, J. M., Synthesis, Characterization, and Variable-Temperature NMR Studies of Silver(I) Complexes for Selective Nitrene Transfer. *Inorg. Chem.* **2017**, *56*, 6725-6733.

51. Scamp, R. J.; Jirak, J. G.; Dolan, N. S.; Guzei, I. A.; Schomaker, J. M., A General Catalyst for Site-Selective C(sp<sup>3</sup>)-H Bond Amination of Activated Secondary over Tertiary Alkyl C(sp<sup>3</sup>)-H Bonds. *Org. Lett.* **2016**, *18*, 3014-3017.

52. Huang, M.; Paretsky, J.; Schomaker, J. M., Rigidifying Ag(I) Complexes for Selective Nitrene Transfer. *ChemCatChem* **2020**, *12*, 3076-3081.

53. Corbin, J. R.; Schomaker, J. M., Tunable differentiation of tertiary C-H bonds in intramolecular transition metal-catalyzed nitrene transfer reactions. *Chem. Commun.* **2017**, *53*, 4346-4349.

54. Scamp, R. J.; Scheffer, B.; Schomaker, J. M., Regioselective differentiation of vicinal methylene C-H bonds enabled by silver-catalysed nitrene transfer. *Chem. Commun.* **2019**, *55*, 7362-7365.

55. Ju, M.; Huang, M.; Vine, L. E.; Dehghany, M.; Roberts, J. M.; Schomaker, J. M., Tunable catalyst-controlled syntheses of  $\beta$ - and  $\gamma$ -amino alcohols enabled by silver-catalysed nitrene transfer. *Nat. Catal.* **2019**, *2*, 899-908.

56. Fu, Y.; Liu, P.; Zerull, E. E.; Schomaker, J. M.; Liu, P., Origins of Catalyst-Controlled Selectivity in Ag-Catalyzed Regiodivergent C-H Amination. *J. Am. Chem. Soc.* **2022**, *144*, 2735-2746.

57. Dias, H. V. R.; Wang, Z.; Jin, W., Synthesis and Chemistry of [Hydrotris(3,5-bis(trifluoromethyl)pyrazolyl)borato]silver(I) Complexes. *Inorg. Chem.* **1997**, *36*, 6205-6215.

58. Gómez-Emeterio, B. P.; Urbano, J.; Díaz-Requejo, M. M.; Pérez, P. J., Easy Alkane Catalytic Functionalization. *Organometallics* **2008**, *27*, 4126-4130.

59. Liao, K.; Pickel, T. C.; Boyarskikh, V.; Bacsa, J.; Musaev, D. G.; Davies, H. M. L., Site-selective and stereoselective functionalization of non-activated tertiary C-H bonds. *Nature* **2017**, *551*, 609-613.

60. Arenas, I.; Fuentes, M. Á.; Álvarez, E.; Díaz, Y.; Caballero, A.; Castillón, S.; Pérez, P. J., Syntheses of a Novel Fluorinated Trisphosphinoborate Ligand and Its Copper and Silver Complexes. Catalytic Activity toward Nitrene Transfer Reactions. *Inorg. Chem.* **2014**, *53*, 3991-3999.

61. Campos, J.; Goforth, S. K.; Crabtree, R. H.; Gunnoe, T. B., Metal-free amidation of ether sp<sup>3</sup> C-H bonds with sulfonamides using PhI(OAc)<sub>2</sub>. *RSC Adv.* **2014**, *4*, 47951-47957.

62. Llaveria, J.; Beltrán, Á.; Díaz-Requejo, M. M.; Matheu, M. I.; Castillón, S.; Pérez, P. J., Efficient Silver-Catalyzed Regio- and Stereospecific Aziridination of Dienes. *Angew. Chem., Int. Ed.* **2010**, *49*, 7092-7095.

63. Llaveria, J.; Beltrán, Á.; Sameera, W. M. C.; Locati, A.; Díaz-Requejo, M. M.; Matheu, M. I.; Castillón, S.; Maseras, F.; Pérez, P. J., Chemo-, Regio-, and Stereoselective Silver-Catalyzed Aziridination of Dienes: Scope, Mechanistic Studies, and Ring-Opening Reactions. *J. Am. Chem. Soc.* **2014**, *136*, 5342-5350.

64. Rodríguez, M. R.; Besora, M.; Molina, F.; Maseras, F.; Díaz-Requejo, M. M.; Pérez, P. J., Intermolecular Allene Functionalization by Silver-Nitrene Catalysis. *J. Am. Chem. Soc.* **2020**, *142*, 13062-13071.

65. Fructos, M. R.; Álvarez, E.; Díaz-Requejo, M. M.; Pérez, P. J., Selective Synthesis of N-Substituted 1,2-Dihydropyridines from Furans by Copper-Induced Concurrent Tandem Catalysis. *J. Am. Chem. Soc.* **2010**, *132*, 4600-4607.

66. Li, Z.; Conser, K. R.; Jacobsen, E. N., Asymmetric alkene aziridination with readily available chiral diimine-based catalysts. *J. Am. Chem. Soc.* **1993**, *115*, 5326-5327.

67. Evans, D. A.; Bilodeau, M. T.; Faul, M. M., Development of the Copper-Catalyzed Olefin Aziridination Reaction. *J. Am. Chem. Soc.* **1994**, *116*, 2742-2753.

68. Li, Z.; Quan, R. W.; Jacobsen, E. N., Mechanism of the (Diimine)copper-Catalyzed Asymmetric Aziridination of Alkenes. Nitrene Transfer via Ligand-Accelerated Catalysis. *J. Am. Chem. Soc.* **1995**, *117*, 5889-5890.

69. Liang, J.-L.; Yuan, S.-X.; Chan, P. W. H.; Che, C.-M., Chiral rhodium(II,II) dimers catalyzed enantioselective intramolecular aziridination of sulfonamides and carbamates. *Tetrahedron Lett.* **2003**, *44*, 5917-5920.

70. Jin, L.-M.; Xu, X.; Lu, H.; Cui, X.; Wojtas, L.; Zhang, X. P., Effective Synthesis of Chiral N-Fluoroaryl Aziridines through Enantioselective Aziridination of Alkenes with Fluoroaryl Azides. *Angew. Chem., Int. Ed.* **2013**, *52*, 5309-5313.

71. Ju, M.; Weatherly, C. D.; Guzei, I. A.; Schomaker, J. M., Chemo- and Enantioselective Intramolecular Silver-Catalyzed Aziridinations. *Angew. Chem., Int. Ed.* **2017**, *56*, 9944-9948.

72. Milczek, E.; Boudet, N.; Blahey, S., Enantioselective C-H amination using cationic ruthenium(II)-pybox catalysts. *Angew. Chem., Int. Ed.* **2008**, *47*, 6825-6828.

73. Zalatan, D. N.; Du Bois, J., A Chiral Rhodium Carboxamidate Catalyst for Enantioselective C-H Amination. *J. Am. Chem. Soc.* **2008**, *130*, 9220-9221.

74. Ju, M.; Zerull, E. E.; Roberts, J. M.; Huang, M.; Guzei, I. A.; Schomaker, J. M., Silver-Catalyzed Enantioselective Propargylic C-H Bond Amination through Rational Ligand Design. *J. Am. Chem. Soc.* **2020**, *142*, 12930-12936.